Measurement of gravitational spin-orbit coupling in a binary pulsar system

I. H. Stairs,[1] S. E. Thorsett,[2] and Z. Arzoumanian[3]

[1]*Department of Physics and Astronomy, University of British Columbia, 6224 Agricultural Road, Vancouver, BC V6T 1Z1, Canada**

[2]*Dept. of Astronomy & Astrophysics, University of California, Santa Cruz, CA 95064*

[3]*USRA, Laboratory for High-Energy Astrophysics, NASA-GSFC, Code 662, Greenbelt, MD 20771*

(Dated: August 25, 2004)

In relativistic gravity, a spinning pulsar will precess as it orbits a compact companion star. We have measured the effect of such precession on the average shape and polarization of the radiation from PSR B1534+12. We have also detected, with limited precision, special-relativistic aberration of the revolving pulsar beam due to orbital motion. Our observations fix the system geometry, including the misalignment between the spin and orbital angular momenta, and yield a measurement of the precession timescale consistent with the predictions of General Relativity.

PACS numbers: 04.80.Cc,97.60.Gb,97.80.Fk,95.85.Bh

1. INTRODUCTION

Parallel transport of the angular momentum of a gyroscope moving in curved spacetime leads to geodetic precession [1]. In the solar system, the only observed example is precession of the Earth-Moon system as it orbits the Sun [2]. The recently launched Gravity Probe B experiment plans to measure the geodetic precession of a gyroscope in Earth orbit as well as its gravitomagnetic Lense-Thirring precession [3].

Binary pulsar systems are important laboratories for gravitational physics [4], in part because the strong self-gravity of neutron stars ($GM/Rc^2 \sim 0.2$) raises the possibility of deviations as large as order unity in some alternate gravity theories—even theories that agree with general relativity (GR) in weak-field tests [5]. Immediately after the discovery of the first binary pulsar, PSR B1913+16 [6], it was realized that geodetic precession could lead to variations in the path of the observer's line of sight across the pulsar's magnetic pole, and hence changes in the radiation pattern at Earth [7]. Recently, the anticipated pulse-profile variations have been observed, in good qualitative agreement with predictions [8–10], but uncertainties in the intrinsic beam shape prevent a quantitative measurement of the precession rate.

Here we describe observations of the double-neutron-star system PSR B1534+12, in which precession is changing the observed pulsar profile by about 1% per year [11, 12]. We outline a new, general technique for combining measurements of long-term quasisecular variations caused by geodetic precession with those of periodic variations induced by special relativistic aberration modulated by orbital motion. Together, the observations allow a quantitative estimate of the precession rate, independent of the unknown pulsar beam shape. Although the precision is still low, we show that this model-independent precession rate is consistent with the predicted rate in GR. The polarization properties of the pulsar signal are also changing: with the additional assumption that the magnetic field structure is dipolar, we can determine the angles between the spin and orbital angular momenta and the line of sight to the pulsar.

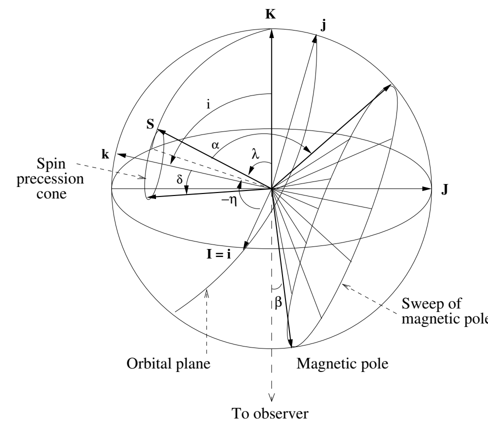

FIG. 1: The spin and orbital geometry we derive for PSR B1534+12, after [4]. The vectors **I** and **J** denote the plane of the sky, while **i** and **j** show the plane of the pulsar orbit. The pulsar spin axis at the current epoch is **S** and the orbital angular momentum direction is **k**; the precession cone with opening (misalignment) angle δ is shown. The angle between **S** and the line of sight is ζ; the supplemental angle $\lambda \equiv \pi - \zeta$ is shown. The angle between **S** and the magnetic pole is α, and $\beta = \zeta - \alpha$ is the minimum impact angle of the magnetic pole on the line of sight. A second cone indicates the sweep of the magnetic pole at the current epoch. The projection of **S** on the plane of the sky (indicated by the dashed line) provides angle η, measured counterclockwise from the ascending node; $-\eta$ is shown. Spherical geometry gives $\cos\delta = -\sin i \sin\lambda \sin\eta + \cos\lambda \cos i$.

The spin and orbital geometry is shown in Fig. 1. The pulsar spin axis **S** will precess around the total angular momentum, which is very well approximated by the orbital angular momentum direction **k**. This precession will cause potentially detectable periodic variations of the projection of **S** on the plane of the sky, and on the inclination of **S** with respect to the observer. In GR, the time averaged precession rate of the pulsar can be written [7]:

$$\Omega_1^{\rm spin} = \frac{1}{2}\left(\frac{GM_\odot}{c^3}\right)^{2/3}\left(\frac{P_{\rm b}}{2\pi}\right)^{-5/3}\frac{m_2(4m_1+3m_2)}{(1-e^2)(m_1+m_2)^{4/3}}, \tag{1}$$

where G is Newton's constant, $M_\odot$ is the mass of the Sun, c is the speed of light, m_1 and m_2 are the pulsar and companion masses, respectively, $P_{\rm b}$ is the orbital period, and e is the eccentricity. A description in generalized theories of gravity is given in [4]. For PSR B1534+12, using the stellar masses determined through high-precision timing [13], the precession rate predicted by GR is 0.51° /yr.

2. OBSERVATIONS AND ANALYSIS

Observations were made with the 300-m Arecibo radio telescope, using the "Mark IV" data acquisition system [14] at an observing frequency of 430 MHz. The signal was processed using coherent dedispersion, providing full polarization information as well as a pulse shape unaffected by dispersive smearing in the interstellar medium. Data acquisition details have been described elsewhere [13].

The data span the interval from mid-1998 to mid-2003, incorporating some 400 hours of observing time. The pulsar was observed biweekly or monthly. The observed signal strength varied widely because of interstellar scintillation; only epochs with high signal-to-noise ratio were used here. Campaigns of roughly 12 contiguous observing days were also conducted every summer except 2002.

The cumulative pulse profile from the representative 2001 June epoch is shown in Fig. 2. Here we also show a fit of the linear polarization to the standard "rotating vector model" (RVM) [15], in which the position angle of linear polarization ψ is assumed to be parallel to the plane of curvature of magnetic dipole field lines rotating with the star, giving

$$\tan\left[\psi\left(\phi\right)-\psi_0\right] = \frac{\sin\alpha\sin\left(\phi-\phi_0\right)}{\cos\alpha\sin\zeta-\sin\alpha\cos\zeta\cos\left(\phi-\phi_0\right)}, \tag{2}$$

where ϕ is the pulse phase, ϕ_0 and ψ_0 are constants, α is the magnetic inclination angle, and ζ is the angle between **S** and the line of sight.

The position angle sweep is observed over most of the pulsar period, and the model fit is generally good. There are strong deviations from the model near the pulse peak, as is often seen for "core" profile components [16]. We exclude this region from our fits. The data are consistent with a roughly orthogonal rotator model, with $\alpha = 102.8 \pm 0.5°$ and the line of sight passing between the magnetic pole and the stellar equator, within a few degrees of the magnetic pole. We also consider the time evolution of α and the impact parameter of the line of sight on the magnetic pole β, using cumulative profiles

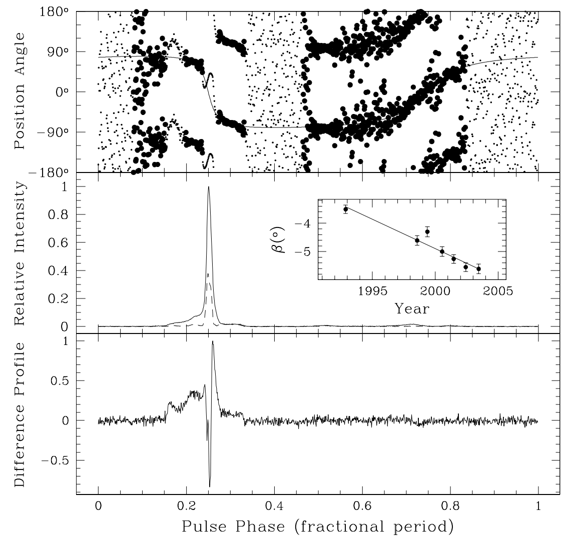

FIG. 2: Top panel: the position angle of linear polarization in 2001 June, measured clockwise on the plane of the sky (the convention in [4]), with best fit rotating vector model (RVM) overlaid. Only the position angle points indicated by large dots were used in the RVM fit; these were weighted by their uncertainties, with a small uncertainty added in quadrature to account for deviations from the RVM. Middle panel: total intensity (solid) and linear polarization (dashed) profiles in 2001 June. This profile is very similar in shape to our "reference" profile P_0. Inset: evolution of impact angle β with time. Bottom panel: "Difference" profile P_1, representing essentially the time-derivative of the observed profile.

from each campaign, one especially strong biweekly observation, and an earlier coherently-dedispersed profile from observations with the "Mark III" data acquisition system [17]. As expected, the data are consistent with no evolution of α. However, as shown in Fig. 2, β is changing with time, at a rate $d\beta/dt = -0.21 \pm 0.03°/{\rm yr}$, resulting in a larger impact parameter at later times. This change in β is direct evidence of geodetic precession, and can be related to the system geometry and precession rate in a simple fashion [4]: $d\beta/dt = \Omega_1^{\rm spin}\cos\eta\sin i$ (see Fig. 1).

The *shape* of the profile is also changing with time and orbital phase, allowing a completely independent probe of the precession. Secular changes in the profile were first noticed at 1400 MHz [11], but evolution of the 430-MHz emission only became apparent with coherently dedispersed observations [12]. Shape variations are more difficult to connect directly to the precession rate than polarization changes. It can be done with an assumed model of the beam shape, as has been attempted for PSR B1913+16 [9, 10, 18], but in that case the true beam shape is still debated and the results are therefore less than satisfactory.

Here we note that it is possible to make a model-independent precession estimate by also measuring the orbital modulation of the profile shape caused by aberration—a special-relativistic effect independent of strong-field gravity. Aberration shifts the observed angle between the line of sight and spin axis by an amount [4]:

$$\delta_{\rm A}\zeta = \frac{\beta_1}{\sin i}\left[-\cos\eta\, S\left(u\right) + \cos i \sin\eta\, C\left(u\right)\right], \qquad (3)$$

where $\beta_1 \equiv nx/\sqrt{(1-e^2)}$ is the characteristic velocity of the pulsar, with the orbital frequency $n \equiv 2\pi/P_b$, the projected semimajor axis $x \equiv a_1 \sin i/c$, and the eccentricity e all available from timing data, and where $C(u) \equiv \cos[\omega + A_e(u)] + e\cos\omega$ and $S(u) \equiv \sin[\omega + A_e(u)] + e\sin\omega$ are functions of the time-dependent angle of periastron passage ω and the eccentric anomaly u through the true anomaly $A_e\left(u\right) \equiv 2\arctan\left[\left(\frac{1+e}{1-e}\right)^{1/2}\tan\frac{u}{2}\right]$.

Now let $F(\zeta)$ be any function defined on the observed pulsar signal that depends on the viewing angle (such as integrated intensity, component width, polarization fraction, etc.). For small changes in the impact parameter, we Taylor-expand $F(\zeta) \approx F(\zeta_0) + \zeta F'$ where prime denotes derivative with respect to ζ. The effects of aberration and precession can then be written

$$\delta_{\rm A}F = F'\frac{\beta_1}{\sin i}\left[-\cos\eta\, S\left(u\right) + \cos i \sin\eta\, C\left(u\right)\right], \qquad (4)$$

$$\frac{dF}{dt} = F'\Omega_1^{\rm spin}\sin i\cos\eta. \qquad (5)$$

The unknown beam shape enters only through F', which can be eliminated by dividing these two equations. Measurements of both the orbital variation of F and its secular drift thus allow $\tan\eta$ and $\Omega_1^{\rm spin}$ to be determined in a model independent way.

For PSR B1534+12, we have measured the evolution of the total intensity profile (Fig. 3). The strongest data scans from the annual campaigns were averaged into 12 orbital phase bins, and analyzed together with the strong biweekly scans. Profiles with unusually low signal-to-noise ratios or suspect calibrations were discarded. We used standard principal component (PC) analysis techniques [19] to derive orthogonal "reference" (P_0) and "difference" (P_1) profiles that completely described the profile evolution; P_1 and a single-epoch profile very similar to P_0 are shown in Fig. 2. The pulse profile P of each observation is well modeled as a linear combination $P = c_0P_0 + c_1P_1$. Because the overall amplitude varied with scintillation, we chose as our observable quantity F the ratio c_1/c_0. The PC analysis provided estimates of c_0, c_1, and their uncertainties, which we independently checked through a frequency-domain cross-correlation technique in which a linear combination of the two profiles was fit in an iterative manner. Finally, we simulated the cross-correlation analysis to assess its sensitivity to systematic errors induced by imperfect calibration or polarization cross-coupling, finding that such problems should be negligible in our dataset.

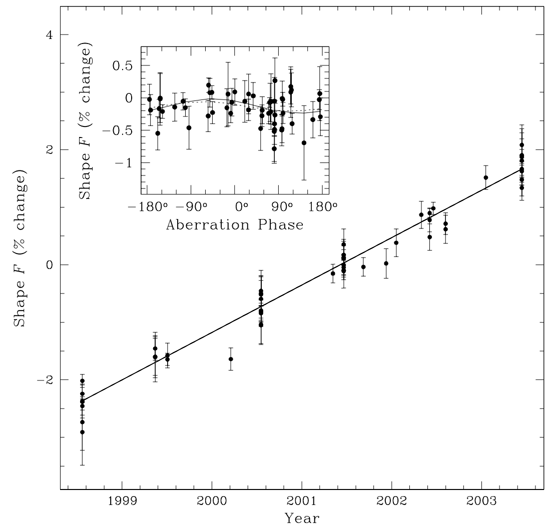

FIG. 3: The shape parameter $F = c_1/c_0$ (see text) is shown as a function of date in the main panel and aberration phase (essentially the true anomaly corrected for the advance of periastron) in the inset. The best-fit model is shown by the solid line in each panel, and in the orbital-phase plot, the GR prediction based on the RVM model is indicated by the dotted line. We have included a small error in quadrature with the measurement errors to account for smearing caused by averaging over a range of orbital phase. To account for systematic errors, variable data quality, and uneven time sampling, we have used a bootstrap analysis [19] to estimate the uncertainties on model parameters. The resulting values and uncertainties are in good agreement with estimates obtained by scaling measurement errors to obtain a reduced-χ^2 of 1.

The secular trend in F is evident in Fig. 3. This corresponds to a decrease in the intensity of the core region of the profile relative to the lower level emission in the wings, consistent with early indications from 1400 MHz data, and as expected if precession is moving our line of sight away from the magnetic pole, as indicated by the polarization analysis above. The residuals after removing the best fit line are shown as a function of orbital phase. A simultaneous linear fit of F as a function of date and of $S(u)$ and $C(u)$ gives the constraints $\Omega_1^{\rm spin}\sin^2 i = 0.42^{+0.46}_{-0.15}\,^\circ/{\rm yr}$ and $\Omega_1^{\rm spin}\sin i\tan i\cot\eta = 0.42^{+0.49}_{-0.16}\,^\circ/{\rm yr}$ (68% confidence), where we have used $\beta_1 = 0.67\times10^{-3}$. A fit of F only as a function of date yields a χ^2 value that is 15% higher than that for the full fit.

3. DISCUSSION

We have observed both long- and short-term variations in the pulse shape of PSR B1534+12, as expected from geodetic precession and aberration. Assuming a dipolar field geometry and GR, the impact parameter change $d\beta/dt = \Omega_1^{\rm spin} \cos\eta \sin i = -0.21 \pm 0.03^\circ$/yr yields a measurement of the previously unknown angle $\eta = \pm 115.0 \pm 3.8^\circ$. Using the pulse timing value $\sin i = 0.975$ [13] but making no assumptions about the validity of the RVM, our measured pulse profile variations yield, using equations 4 and 5, the consistent result $\eta = \pm 103 \pm 10^\circ$. Moreover, we may now solve for the precession rate, $\Omega_1^{\rm spin} = 0.44^{+0.48}_{-0.16}\,^\circ$/yr (68% confidence) or $\Omega_1^{\rm spin} = 0.44^{+4.6}_{-0.24}\,^\circ$/yr (95% confidence). This value compares well with the GR-predicted rate of $\Omega_1^{\rm spin} = 0.51^\circ$/yr.

The misalignment angle δ between the spin and orbital angular momenta can also be constrained. The angle λ is known from the polarization studies. Only the absolute values of $\sin\eta$ and $\cos i$ are known, but our profile fit requires that $\cos i \tan\eta > 0$. Therefore there are two possible geometries: $i = 77.2^\circ$ and $\eta = -115^\circ$, which gives $\delta = 25.0 \pm 3.8^\circ$, or $i = 102.8^\circ$ and $\eta = 115^\circ$, which gives $\delta = 155.0 \pm 3.8^\circ$. Both give identical results for precession in GR. As the angular momenta were almost certainly aligned before the second supernova, the smaller misalignment value is favored on astrophysical grounds [20]. The preferred geometry then has $i = 77.2^\circ$, $\eta = -115.0 \pm 3.8^\circ$, and $\delta = 25.0 \pm 3.8^\circ$ (Fig 1). The misalignment angle can be used to constrain mass loss and asymmetry in the second supernova. A full analysis will be published elsewhere, along with a study of the two-dimensional beam geometry of PSR B1534+12.

Although the precision is, as yet, limited, this is the first beam-model-independent measurement of the precession rate of a binary pulsar and reconstruction of the full three dimensional geometry of a binary pulsar system, including the misalignment angle. Future prospects for improvement include direct estimation of the angle η by combining scintillation studies [21] with polarimetry [4]. The derived geometry also allows us to predict the effects of aberration on the pulse timing [4]; this will in principle allow more precise timing tests of GR in future.

We emphasize that the general technique of combining observations on the orbital and precessional timescales to make model independent precession rate estimates is potentially far more general than the particular example given here. An especially interesting prospect is the recently discovered highly relativistic system PSR J0737−3039 [22]; with β_1 nearly twice as large as that of B1534+12, and a predicted precession timescale for the recycled pulsar of only 75 years, both effects will be quickly measured for this new system.

The Arecibo Observatory is operated by Cornell University under a cooperative agreement with the NSF. IHS is supported by an NSERC Discovery Grant. SET acknowledges support from the NSF. ZA is supported by a NASA grant. We thank D. Nice for his contributions to the software that made this work possible, J. Taylor for significant help and encouragement in the early stages, and numerous colleagues for assistance with observations. We also thank the Arecibo Scheduling Advisory Committee for its longstanding support of this project.

---

* Electronic address: stairs@astro.ubc.ca; URL: http://www.astro.ubc.ca/people/stairs/

[1] W. de Sitter, Mon. Not. R. Astron. Soc. **77**, 155 (1916).
[2] J. G. Williams, X. X. Newhall, and J. O. Dickey, Phys. Rev. D **53**, 6730 (1996).
[3] S. Buchman, C. W. F. Everitt, B. Parkinson, J. P. Turneaure, D. DeBra, D. Bardas, W. Bencze, R. Brumley, D. Gill, G. Gutt, et al., Adv. Space Res. **26**, 1177 (2000).
[4] T. Damour and J. H. Taylor, Phys. Rev. D **45**, 1840 (1992).
[5] T. Damour and G. Esposito-Farese, Phys. Rev. D **54**, 1474 (1996).
[6] R. A. Hulse and J. H. Taylor, Astrophys. J. **195**, L51 (1975).
[7] T. Damour and R. Ruffini, C. R. Acad. Sc. Paris, Serie A **279**, 971 (1974).
[8] J. M. Weisberg, R. W. Romani, and J. H. Taylor, Astrophys. J. **347**, 1030 (1989).
[9] M. Kramer, Astrophys. J. **509**, 856 (1998).
[10] J. M. Weisberg and J. H. Taylor, Astrophys. J. **576**, 942 (2002).
[11] Z. Arzoumanian, Ph.D. thesis, Princeton University (1995).
[12] I. H. Stairs, S. E. Thorsett, J. H. Taylor, and Z. Arzoumanian, in *Pulsar Astronomy - 2000 and Beyond, IAU Colloquium 177*, edited by M. Kramer, N. Wex, and R. Wielebinski (Astronomical Society of the Pacific, San Francisco, 2000), pp. 121–124.
[13] I. H. Stairs, S. E. Thorsett, J. H. Taylor, and A. Wolszczan, Astrophys. J. **581**, 501 (2002).
[14] I. H. Stairs, E. M. Splaver, S. E. Thorsett, D. J. Nice, and J. H. Taylor, Mon. Not. R. Astron. Soc. **314**, 459 (2000).
[15] V. Radhakrishnan and D. J. Cooke, Astrophys. Lett. **3**, 225 (1969).
[16] J. M. Rankin, Astrophys. J. **274**, 333 (1983).
[17] Z. Arzoumanian, J. A. Phillips, J. H. Taylor, and A. Wolszczan, Astrophys. J. **470**, 1111 (1996).
[18] M. Kramer, in *IX Marcel Grossmann Meeting* (World Scientific, 2002).
[19] W. H. Press, S. A. Teukolsky, W. T. Vetterling, and B. P. Flannery, *Numerical Recipes: The Art of Scientific Computing, 2^{nd} edition* (Cambridge University Press, Cambridge, 1992).
[20] M. Bailes, Astron. Astrophys. **202**, 109 (1988).
[21] S. Bogdanov, M. Pruszunska, W. Lewandowski, and A. Wolszczan, Astrophys. J. **581**, 495 (2002).
[22] M. Burgay, N. D'Amico, A. Possenti, R. N. Manchester, A. G. Lyne, B. C. Joshi, M. A. McLaughlin, M. Kramer, J. M. Sarkissian, F. Camilo, et al., Nature **426**, 531 (2003).